Spectroscopic (FT-IR, FT-Raman), first order hyperpolarizability, NBO and HOMO-LUMO analysis of Z)-3-(2,4-dichlorophenyl)1-(1H- imidazol-1-yl)prop-2-en-1-one

Article · August 2020

Dr.Ramasamy Naicker Karunathan
Dr. N.G.P. Arts and Science College

Spectroscopic (FT-IR, FT-Raman), first order hyperpolarizability, NBO and HOMO-LUMO analysis of Z)-3-(2,4-dichlorophenyl)1-(1H-imidazol-1-yl)prop-2-en-1-one

S. Arulappan, R.RajMuhamed, A. IshaqAhamed, R.Karunathan, D.Prabha, S.Krishnaveni

Abstract: The Fourier Transform Infrared (FT-IR) and FT-Raman Spectra of ((Z)-3-(2,4-dichlorophenyl)-1-(1H-imidazol-1-yl)prop-2-en-1-one (1) have been recorded in the regions 4000-100 and 4000-450cm^{-1}, respectively. A complete assignment and analysis of the fundamental vibrational modes of the molecule were carried out. The observed fundamental modes have been compared with the harmonic vibrational frequencies computed using DFT (B3LYP) method by employing 6-311++G(d,p) basis sets. The vibrational studies were interpreted in terms of potential energy distribution. The first order hyperpolarizability (β_0) and related properties (α, μ and $\Delta\alpha$) of this molecular system were calculated using B3LYP/6-311++G(d,p) method based on the finite-field approach. Stability of the molecule arising from hyperconjugative interactions and charge delocalization have been analyzed using natural bond orbital (NBO) analysis.. Molecular electrostatic potential (MEP) and HOMO-LUMO energy levels were also constructed.

Index Terms: DFT, FT-IR, FT-Raman, HOMO-LUMO, MEP, NLO.

1. INTRODUCTION

Imidazole derivatives have attracted significant interest in recent time for their usefulness in synthetic heterocyclic chemistry, analytical and pharmacology. They are a highly polar and have a calculated dipole moment of 3.61D. It is 5- membered nitrogen containing heterocyclic ring, which are soluble in both organic and inorganic polar solvents. They are amphoteric in nature and aromatic in character due to the presence of 6 -electrons.The nitrogen attached with the hydrogen has a lone pair of electrons bringing the required 6 -electrons for aromaticity. The hydrogen atom can be located on either of the two nitrogen atoms due to resonance structures of imidazole [1]. A literature survey of imidazole derivatives show that they posses antimicrobial, anti-inflammatory, analgesic, anti-tubercular and anticancer activities. Further possible improvements in their activity can be achieved by slight modifications in the substituent on the basic imidazole nucleus. By virtue of having structural similarity with histidine, imidazole compound can bind with protein molecules with ease when compared to the some other heterocyclic moieties membranes, without interference with sterols and sterol esters. Recently various new drugs developed using imidazoles derivatives have shown better effect and less toxicity.

- *Arulappan S, Research Scholar, Department of Physics, Jamal Mohamed College(Bharatyhidasan University), Tiruchirappalli 620020, Tamil Nadu, India*
- *RajMuhamed R, Associate Professor, Department of Physics, Jamal Mohamed College, Tiruchirappalli 620020, Tamil Nadu, India*
- *Ishaq Ahamed A, Associate Professor, Department of Physics, Jamal Mohamed College, Tiruchirappalli 620020, Tamil Nadu, India*
- *Karunathan R, Assistant Professor, Department of Physics, Dr.NGP. College of Arts and Science, Coimbatore – 641 014, Tamil Nadu, India*
- *Prabha D, Assistant Professor, Department of Physics, PSG College of Arts & Science, Coimbatore – 641 014,Tamil Nadu, Indi*
- *Krishnaveni S, Research Scholar, Department of Physics*, PSG College of Arts & Science, Coimbatore – 641 014,Tamil Nadu, India

2. Synthesis of (Z)-3-(2,4-dichlorophenyl)1-(1H-imidazol-1-yl)prop-2-en-1-one

A mixture of N-acetyl imidazole (0.01mmol) and 2,4-dicholorobenzaldehyde(0.01mmol) was dissolved in 20 ml of ethanol, cooled to 5 -10 °C in an ice bath. A cold aqueous sodium hydroxide solution (10 ml, 10%, wt/v) was added drop wise to the reaction mixture under stirring and after the addition, the stirring was continued for 6 h under ice-cold condition. A flocculent precipitate formed in the process was filtered, washed with cold water, and recrystallized from ethanol. The components of the reaction mixture were analyzed by TLC and the product was separated from a silica column.

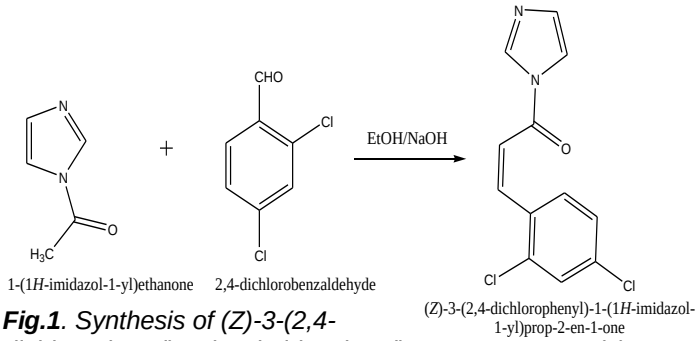

***Fig.1**. Synthesis of (Z)-3-(2,4-dichlorophenyl)-1-(1H-imidazol-1-yl)prop-2-en-1-one (1) from the crossed aldol condensation of N-acetylimidazole with 2,4-dichloronitrobenzaldehyde*

2.1 Experimental

The FT-IR spectrum of the synthesis compound 3BSC was recorded in the region 4000-450 cm^{-1} in evacuation mode using a KBr pellet technique with 1.0 cm^{-1} resolution on a PERKIN ELMER FT-IR spectrophotometer. The FT-

Raman spectrum of the title molecule was recorded in the region 4000-100 cm^{-1} in a pure mode using Nd:YAG Laser of 100 mW with 2cm^{-1} resolution on a BRUCKER RFS 27 at SAIF, IIT, Chennai, India. Carbon(13C) NMR and Proton (1H) NMR spectra were recorded in DMSO-d6 using TMS as an internal standard on a Bruker high-resolution NMR spectrometer at 400 MHz at CAS in Crystallography & Biophysics, University of Madras, Chennai, India. The ultraviolet absorption spectrum of the sample is examined in the range 200-600 nm using UV-1700 series recording spectrometer.

2.2. Computational method

Quantum chemical density functional computations were carried out at the Becke3-Lee-Yang-parr (B3LYP) level with 6-311++G(d,p) basis set using Gaussian 09W program package [2] to get a clear knowledge of optimized parameters. The optimized molecular structure (Fig. 2) is used for the computation of vibrational frequencies, Raman activities and IR intensities with the Gaussian 09W software system and GaussView 5.0 [3] molecular visualization program at the same level of theory and basis set. The theoretical vibrational assignments of the 3BSC molecule using percentage potential energy distribution (PED) have been done with the VEDA program [4]. In order to understand the electronic properties, the theoretical UV-Vis spectra have been investigated by TD-DFT method with 6-311++G(d,p) basis set for the gas phase. The proton and carbon NMR chemical shift were calculated with gauge-including atomic orbital (GIAO) approach [5] by applying B3LYP/6-311++G(d,p) method of the title molecule and compared with the experimental NMR spectra. Molecular docking (ligandprotein) simulations have been performed by using auto Dock 4.2.6 free software package. The calculated Raman activities (Si) with Gaussian 09W program have been converted to relative Raman Intensities (Ii) using the following relationship obtained from the basic theory of Raman scattering [6], [7],

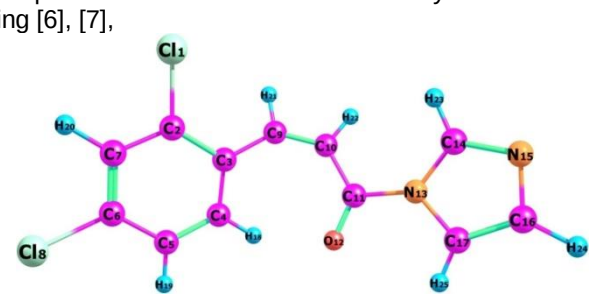

Fig. 2. Optimized geometric structure with atoms numbering of (Z)-3-(2,4-dichlorophenyl)1-(1H-imidazol-1-yl)prop-2-en-1-one

$$Ii = f\,(v_0 - v_i)^4 s_i \qquad v_i[1 - \exp{-hc\,v_i}]/kT$$

Where v_0 is the laser exciting frequency in cm-1, v_i is the vibrational frequency of the ith normal mode, h, c and k are universal constants and f is a suitably chosen common scaling factor for all peak intensities.

3. RESULTS AND DISCUSSIONS

3.1 Structural Description

The geometrical optimization was carried out using the B3LYP/6-311++G(d,p) basis set and the optimized molecular structure is as shown in Fig. 2. The bond lengths, bond angles and dihedral angles are presented in Table 1. The optimized parameters were calculated in the gas phase and compared with the XRD results. The statistical linear regression plots between the experimental XRD values and theoretical geometrical parameters, such as bond lengths and angles, showed good agreement, as shown in Table 1. C_{11}-N_{13} manifested the shortest C-N bond length (1.423 Å), while N_{13}-C_{14} displayed the longest C-N bond length (1.431 Å), which is shorter than the normal C-N bond length (1.480 Å). This may be due to the fact that the lone pair interactions of the nitrogen atoms in the imidazole ring may affect the N_{13}-C_{17} (1.393 Å) and N_{15}-C_{16} (1.364 Å) bond lengths and make them shorter than other C-N bonds in the imidazole ring. The distance between O_{12}…and C_{11} is 1.216 Å, which is shorter than the vander Waal's radius (2.75 Å). This suggests the possibility of hydrogen bonding (N_{13}-C_{11}….O_{12}). The bond lengths between Cl_1-C_2 and C_6-Cl_8 are 1.76 and 1.751 Å, respectively, and they showed a slight deviation from the normal C-Cl bond lengths, possibly due to the Halogen group conjugation. The calculated bond length of C_4-H_{18} is 1.079Å. C_{10}-C_{11} manifested a relatively longer bond length (1.474 Å) than the other C-C bonds. The C-H bond lengths in the phenyl ring vary from 1.081 Å (C_7-H_{20}) to 1.075 Å (C_4-H_{18}) and it seems that the C-H bond lengths in the other rings do not deviate much. The para substituted phenyl ring is planar with a C_5-C_6-Cl_8 chlorophenyl angle of 119.9°. The calculated bond angles C_{10}-C_{11}-O_{12} (126.5°), O_{12}-C_{11}-N_{13} (118.7°) and C_2-C_7-C_6 (118.8°) seem to be consistent with the experimental values.

Table 1

Optimized geometrical parameters of (Z)-3-(2,4-dichlorophenyl)1-(1H-imidazol-1-yl)prop-2-en-1-one obtained by B3LYP/6-311++G(d,p) basis set.

Parameters	Experimental[a]	B3LYP/6-311++G(d,p)	Parameters	Experimental[a]	B3LYP/6-311++G(d,p)
Bond length(Å)			Bond angle(°)		
Cl_1-C_2	-	1.76	Cl_1-C_2-C_3	-	121.1
C_2-C_3	1.415	1.413	Cl_1-C_2-C_7	-	116.5
C_2-C_7	1.384	1.388	C_3-C_2-C_7	121.97	122.4
C_3-C_4	1.408	1.408	C_2-C_3-C_4	117.4	116.4
C_3-C_9	1.477	1.464	C_2-C_3-C_9	119.60	119.5
C_4-C_5	1.389	1.388	C_2-C_7-C_6	118.6	118.8
C_4-H_{18}	0.930	1.079	C_2-C_7-H_{20}	119.7	120.4
C_5-C_6	1.355	1.39	C_4-C_3-C_9	123.55	124
C_5-H_{19}	0.930	1.082	C_3-C_4-C_5	122.40	122.1
C_6-C_7	1.389	1.391	C_3-C_4-H_{18}	118.8	118.5
C_6-Cl_8	-	1.751	C_3-C_9-C_{10}	129.36	134
C_7-H_{20}	0.930	1.081	C_3-C_9-H_{21}	115.3	112.6
C_9-C_{10}	1.355	1.352	C_5-C_4-H_{18}	119.3	119.4
C_9-H_{21}	0.930	1.085	C_4-C_5-C_6	119.41	119.3

C_{10}-C_{11}	1.477	1.474	C_4-C_5-H_{19}	119.7	120.4
C_{10}-H_{22}	0.930	1.083	C_6-C_5-H_{19}	119.7	120.3
C_{11}-O_{12}	1.216	1.214	C_5-C_6-C_7	120.63	121
C_{11}-N_{13}	1.431	1.423	C_5-C_6-Cl_8	-	119.9
N_{13}-C_{14}	1.431	1.392	C_7-C_6-Cl_8	-	119.1
N_{13}-C_{17}	1.431	1.393	C_6-C_7-H_{20}	120.5	120.8
C_{14}-N_{15}	1.305	1.301	C_{10}-C_9-H_{21}	115.3	113.3
C_{14}-H_{23}	0.930	1.078	C_9-C_{10}-C_{11}	129.36	129.8
N_{15}-C_{16}	1.364	1.388	C_9-C_{10}-H_{22}	115.3	115.4
C_{16}-C_{17}	1.357	1.361	C_{11}-C_{10}-H_{22}	115.3	114.8
C_{16}-H_{24}	0.930	1.078	C_{10}-C_{11}-O_{12}	120.97	126.5
C_{17}-H_{25}	0.930	1.075	C_{10}-C_{11}-N_{13}	112.81	114.8
			O_{12}-C_{11}-N_{13}	118.10	118.7
			C_{11}-N_{13}-C_{14}	128.00	130.2
			C_{11}-N_{13}-C_{17}	125.02	123.8
			C_{14}-N_{13}-C_{17}	104.26	105.9
			N_{13}-C_{14}-N_{15}	112.21	111.9
			N_{13}-C_{14}-H_{23}	123.90	122.6
			N_{13}-C_{17}-C_{16}	104.260	105.7
			N_{13}-C_{17}-H_{25}	123.90	120.9
			N_{15}-C_{14}-H_{23}	123.90	125.4
			C_{14}-N_{15}-C_{16}	104.26	105.6
			N_{15}-C_{16}-C_{17}	106.95	110.8
			N_{15}-C_{16}-H_{24}	123.90	121.1
			C_{17}-C_{16}-H_{24}	127.90	128.1
			C_{16}-C_{17}-H_{25}	127.90	133.3

[a] Taken from Ref [13]

3.2 Vibrational Assignment

The title molecule contains 25 atoms, and it has 69 normal modes of vibration. All the 69 fundamental vibrations are FT-IR and FT-Raman active. The harmonic-vibrational frequencies calculated for the title molecule have been compared with the experimental frequencies and are given in Table 2. The calculated vibrational wave numbers are usually higher than the corresponding experimental quantities because of the combination of electron correlation effects and basis sets deficiencies. Therefore, it is customary to scale down the calculated harmonic wavenumber in order to improve the agreement with the experimental values. After applying a uniform scaling factor, the theoretical calculations agreed well with the experimental data. Vibrational assignments are based on the observations of the animated modes in Gauss View and assignments reported in the literature.

Table 2

Calculated vibrational frequencies (cm^{-1}) assignments of (Z)-3-(2,4-dichlorophenyl)1-(1H-imidazol-1-yl)prop-2-en-1-one based on B3LYP/6-311++G(d,p) basis set.

Mode no	Experimental wave number (cm^{-1})		Theoretical wave number(cm^{-1})		I_{IR} [c]	I_{RAMAN} [d]	Assignments (PED)[a,b]
	FTIR	FT-RAMAN	Unscaled	scaled			
69			3296	3167	2	4	YCH(95)
68			3263	3135	1	3	YCH(97)
67			3248	3122	2	9	YCH(95)
66			3239	3113	11	5	Y CH(97)
65			3219	3094	0	5	YCH(99)
64			3206	3080	0	5	YCH(97)
63			3185	3060	1	5	YCH(99)
62	2935 (m)		3157	3034	1	2	YCH(74)
61	1676 (vs)	1654 (m)	1747	1679	63	10	YOC(76)
60	1581 (vs)	1597 (vs)	1653	1588	90	100	YCC(61)
59			1617	1554	65	79	YCC(36) + β HCC(11)
58	1516 (vs)	1523 (vs)	1576	1515	2	5	YCC(33)
57			1564	1503	8	4	YCC(75)
56	1440 (s)		1503	1444	4	3	β HCC(17)+ YCC(28)
55		1434(s)	1496	1438	100	1	βHCC(16) + YCC(23)+ βHCN(18)
54	1399 (m)		1468	1411	20	3	βHCC(57)
53	1382 (m)		1417	1362	8	8	βHCC(17)
52		1315(s)	1397	1342	21	1	YCC(16) + YNC(15)
51	1283 (vs)		1354	1301	6	16	βHC(35) + YCC(15)
50	1257 (vs)	1256(s)	1307	1256	5	4	βHCC(11) + βHCN(30)
49			1296	1245	1	2	βHCC(23) + YCC(12)
48			1294	1244	59	1	βHCC(12) + βHCN(14)
47			1276	1227	4	0	βHCC(19)
46	1197 (s)		1254	1205	185	0	YNC(14) + βHCN(22)
45	1170 (vs)	1163 (m)	1208	1161	0	4	βHCC(11) + YCC(10)
44	1115 (s)		1167	1121	8	4	YCC(20) + YClC(13)
43	1106 (s)		1125	1081	8	0	YNC(35) + βHCN(30)
42			1118	1075	20	6	YCC(18) + YClC(16)

41			1096	1053	61	5	βHCN(21) + YCC(11)
40		1024 (m)	1062	1021	17	0	βHCC(34) + YClC(21)
39	1042 (s)		1052	1011	6	1	βHCC(14) + βHCN(13) + YCC(14)
38	971 (m)	999(s)	1026	986	1	4	τHCCC(20)
37			995	956	4	0	τHCCC(14)
36			979	941	64	1	βHCN(13) + YCC(13)
35	891 (w)		908	873	0	1	βHCN(60)
34			898	863	27	0	βHCC(13) + τ HCCC(13)
33			891	857	0	0	τHCCH(89)
32	840 (m)		881	847	5	0	τHCCCl(79) + τHCCC(12)
31			850	817	15	0	τHCCC(51)
30	803 (m)		836	803	14	1	τClC(13) + τHCCO(14)
29			815	784	23	1	τHCCC(23) + τCCCCl(10)
28	786 (m)		815	783	5	0	τHCNC(16) + τHCCC(10) + τHCCO(12) + τCCCCl(17)
27			765	735	9	0	τHCNC(89)
26			750	720	7	1	τHCCC(39)
25			709	682	6	0	YCC(2) + YClC(13)
24	653 (m)		684	657	3	3	τHCCC(45)
23	634 (m)		658	633	8	0	τHCNC(67)
22			652	627	5	1	YCC(15) + YClC(13)
21			614	591	1	1	τHCNC(58)
20	586 (m)		603	580	4	0	βHCC(10)
19	525 (m)		560	539	2	0	τHCCC(39)
18			516	496	1	1	YCC(15)
17			468	450	5	3	τHCCC(38)
16	416 (w)		421	405	5	0	-
15			415	399	1	1	βHCC(14) + YClC(13)
14			402	387	3	0	-
13			377	362	2	0	βHCC(11)
12			311	299	7	0	βHCC(43)
11			275	265	1	0	τHCCC(32)
10			226	217	1	0	βHCC(10) + βCCC(16)
9			201	193	0	0	-
8			168	162	0	0	τHCCCl(84)
7			153	147	1	0	τHCCO(19) + τHCCC(11) + τCCCCl(21)
6			138	133	0	0	βHCC(14) + βCCC(10)
5			125	120	1	0	τHCC(25) + τCCCCl(10) + τHCCC(10)
4			70	68	1	0	τHCCC(48)
3			55	53	0	0	τHCCC(27)
2				19	18	0	0	τHCCO(15) + τHCCC(4
1				14	13	0	1	τHCCC(48)

[a]γ-stretching,γ_a-Symmetrical stretching,γ_{as}-asymmetrical stretching, β- inplane bending ,ω- outplane bending, τ-torsion, vs-very strong, s- strong, m-medium, w-weak.
[b]scaling factor : 0.961 for B3LYP/6-311+G(d,p)
[c]Relative absorption intensities normalized with highest peak absorption equal to 100.
[d]Relative Raman intensities normalized to 100.

C-H Vibrations

The presence of C-H stretching vibrations is expected in the region 3100-3000 cm^{-1} which is the characteristic region for the ready identification of C-H [8] stretching vibrations. In this region, the bands are not affected appreciably by the nature of the substituent. The weak band in FT-IR at 2935 cm^{-1} is assigned to C-H stretching vibration and scaled frequency at 3034 cm^{-1}. The bands due to C-H in-plane bending vibrations are somewhat mixed with C-C stretching and are observed in experimental (FT-IR) number of bands from 1440 to 1257 cm^{-1} and B3LYP/6-31 G (d, p) method as a 1444 to 1227 cm^{-1} . Arivazhagan et al [9] have assigned C-H in-plane bending vibrations in the region 1300-1000 cm^{-1} and C-H out-of-plane bending vibrations in the region 1000-750 cm^{-1}. For our title molecule, the strong band observed at 1042 to 786 cm^{-1} respectively in FT-IR spectrum for C-H out-of-plane bending vibrations, the scaled value (B3LYP/6-31 G (d, p) in the region 1052 to 815 cm^{-1}. These C-H vibrations showed good concurrence with scaled values and experimental frequencies.

C-C Stretching Vibrations

Generally the C-C stretching vibrations occur in the region of 1625-1430 cm^{-1} [10]. In the present study, the C-C stretching absorptions occur in between 1581-1516 cm^{-1} which is normally strong band for the title molecule. The calculated values of C-C stretching vibrations are found to be 1588, 1554, 1515 and 1503 cm^{-1} (B3LYP/6-31 G (d, p). Both scaled values and experimental frequencies are in good agreement with the literature data.

C=O and C=N Vibrations

The stretching mode C=O was calculated at 1676 cm^{-1} and assigned to the strong band observed in FT-IR peak spectra at 1679 cm^{-1}. The identifications of C-N stretching frequencies are a rather difficult task, since the mixing of vibrations is possible in this region. The C-N stretching vibrations usually lie in the region 1382-1266 cm^{-1} [8]. The C-N stretching is calculated at 1342 cm^{-1} in FTIR spectrum. The characteristic peak of C=N stretching mode was identified as broad peaks at 1197 in FT-IR spectrum in the figures 3 & 4.The calculated value at 1205 cm^{-1} for the title molecule. Experimental and calculated values are in good agreement with the literature data.

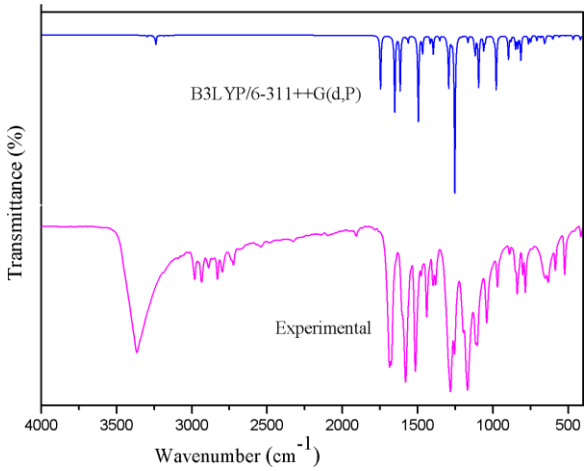

***Fig. 3**. FT- IR spectra of (Z)-3-(2,4-dichlorophenyl)1-(1H-imidazol-1-yl)prop-2-en-1-one. (Experimental, B3LYP/6-311++G(d,p))*

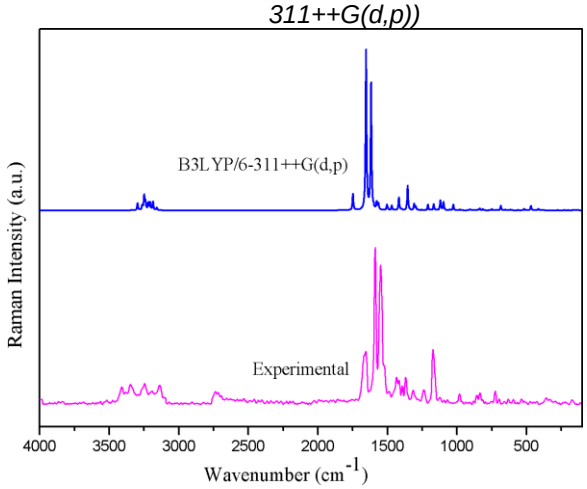

***Fig. 4**. FT-Raman spectra of (Z)-3-(2,4-dichlorophenyl)1-(1H-imidazol-1-yl)prop-2-en-1-one. (Experimental, B3LYP/6-311++G (d,p)*

3.3 NMR Studies

Nuclear magnetic resonance (NMR) spectroscopy can be used to determine the isotropic chemical shifts of atom nucleus in different chemical environment, ionic species in the molecule and the content and purity of a compound [11], [12], [13]. The ^{1}H and ^{13}C NMR isotropic chemical shifts of the title compound were experimentally recorded in chloroform-d. The recorded proton and carbon-13 NMR chemical shift spectra are depicted in Figure 5, 6. The 1H and 13C NMR chemical shifts computed for the title compound were obtained at the B3LYP/6-311G(d,p) level using IEFPCM model and GIAO method in chloroform. The recorded and computed proton and carbon-13 NMR chemical shifts for (Z)-3-(2,4-dichlorophenyl)1-(1H-imidazol-1-yl)prop-2-en-1-one molecule are listed in Table 3. The carbon-13 NMR chemical shifts for the title molecule can be evaluated in the titled carbons. The electronegativity, conjugation and inductive effects can cause an increase in carbon-13 NMR chemical shifts due to polarization of the electron distribution of the molecule. Carbonyl carboxylic acids, imidazole, and aldehyde groups, which are attached by a π-bond to the highly electronegative oxygen atom, give rise to the occurrence of NMR chemical shifts between 160-220 ppm [11-13]. The recorded and computed NMR chemical shift values for C11 carbon atom in imidazole group of the title compound were found at 184.900 ppm and 184.527 ppm, respectively. The NMR chemical shift signals of carbons in aromatic rings can be observed in the region of 100-175 ppm, depending on species of the substituent groups bonded to these carbons [11], [12], [13]. In this connection, the C3, C4, C5, C6, C7, C9, C14, C16 and C17 phenyl carbons in the title compound give rise to NMR resonance signals at the interval of 138.360-111.330 ppm. The computed values for these carbons were obtained in the region of 138.833-110.042 ppm. The saturated sp3 carbon atoms can cause NMR signals in the region of 8-60 ppm of highest field [12]. If these carbons attach an electron-withdrawing or particular group, they shift towards the downfield and give signals at highest chemical shift values, due to a reduction in the electron density [11], [12], [13]. The aromatic ring protons with sp2 hybrid give a large chemical shift at the region of 6.5-8.0 ppm [11-13]. The five identical phenyl protons (H18, H19, H20, H21, H22, H23, H24, and H39) of the title molecule gave rise to a strong singlet NMR signal at 7.41 ppm.

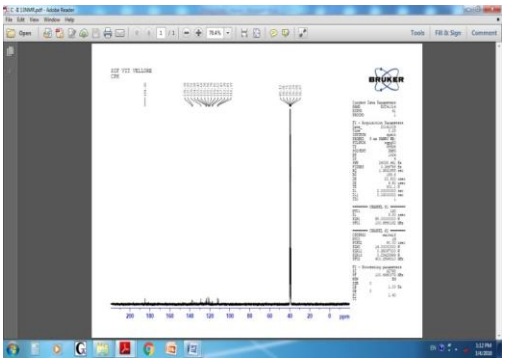

***Fig.5**. ^{13}C NMR spectrum of (Z)-3-(2,4-dichlorophenyl)1-(1H-imidazol-1-yl)prop-2-en-1-one. (Experimental)*

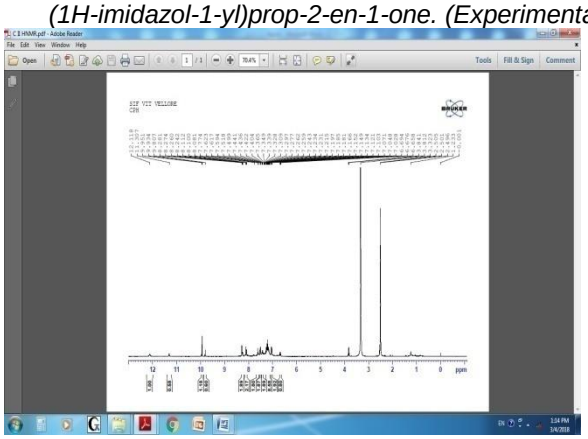

***Fig. 6**. ^{1}H NMR spectrum of (Z)-3-(2,4-dichlorophenyl)1-(1H-imidazol-1-yl)prop-2-en-1-one. (Experimental)*

The computed NMR chemical 286 shift values for these five phenyl protons were obtained at the interval of 7.623-7.774 ppm.

Table 3

Theoretical and experimental ^{13}C and ^{1}H isotropic chemical shifts [with respect to TMS, all values in ppm] for (Z)-3-

(2,4-dichlorophenyl)1-(1H-imidazol-1-yl)prop-2-en-1-one molecule

Atom	Chemical shifts (ppm)	
	Experimental	B3LYP/6-311++G(d,p)
C_{11}	184.900	184.527
C_9	138.360	138.833
C_6	137.000	131.375
C_2	129.010	130.144
C_{14}	124.080	125.685
C_4	123.400	124.802
C_3	122.060	121.191
C_{16}	120.760	120.095
C_7	119.720	117.930
C_5	117.120	117.228
C_{20}	112.610	112.682
C_{17}	111.330	110.042
H_{18}	9.807	9.7535
H_{23}	8.112	8.1194
H_{21}	8.081	7.9376
H_{25}	7.774	7.8916
H_{20}	7.623	7.6869
H_{19}	7.617	7.6045
H_{24}	7.365	7.357
H_{22}	7.309	7.2178
H_{18}	9.807	9.7535

3.4 Frontier Molecular Orbital Analysis

The Frontier Molecular Orbital theory plays an important role in the electric and optical properties. The HOMO is the orbital that primarily acts as an electron donor and the LUMO is the orbital that largely acts as the electron acceptor [14]. The value of the energy separation between the HOMO and LUMO is 4.0551 eV. This electronic absorption corresponds to the transition from the ground to the first excited state and is mainly described by one electron excitation from the highest occupied molecular orbital (HOMO) to the lowest unoccupied molecular orbital (LUMO). HOMO and LUMO orbital not only determine the way in which the molecule interacts with other species, but also their energy gap helps to characterize the chemical reactivity and kinetic stability of the molecule [15] and explains the eventual charge transfer interactions that take place within the molecules. As seen from Fig. 7, in HOMO electrons are mostly localized on chlorine atoms, C=O, C=C and the methoxy group at O_{12}.On the other hand in LUMO electrons are mainly localized on phenyl , C=O, C=C and methoxy group at O_{12}. Both HOMO and LUMO are mostly localized on rings which show that they are p type orbital. For understanding various aspects of pharmacological sciences including drug design and the possible ecotoxicological characteristics of the drug molecules, several new chemical reactivity descriptors have been proposed. Conceptual DFT based descriptors have helped in many ways to understand the structure of the molecules and their reactivity by calculating the chemical potential, global hardness and electrophilicity. Using HOMO and LUMO orbital energies, the ionization energy and electron affinity can be expressed as: $I = - E_{HOMO}$, $A = - E_{LUMO}$, $\eta = (-E_{HOMO} + E_{LUMO})/2$ and $\mu = (E_{HOMO} + E_{LUMO})/2$ [16]. Parr et al. [17] proposed the global electrophilicity power of a ligand as $\omega = \mu^2/2\eta$. This index measures the stabilization in energy when the system acquires an additional electronic charge from the environment. Electrophilicity encompasses both the ability of an electrophile to acquire additional electronic charge and the resistance of the system to exchange electronic charge with the environment. It contains information about both electron transfer (chemical potential) and stability (hardness) and is a better descriptor of global chemical reactivity. The hardness g and chemical potential I are given by the following relations :$\eta = (I - A)/2$ and $\mu = -(I + A)/2$, where I and A are the first ionization potential and electron affinity of the chemical species [18]. For the title compound, E_{HOMO} = -6.9746 eV, E_{LUMO} = -2.9195 eV, Energy gap = HOMO – LUMO = 4.0551 eV, Ionization potential I = 6.9746 eV, Electron affinity A = 2.9195 eV, global hardness g = 2.027 eV, chemical potential μ = 4.94 eV and global electrophilicity = $\mu^2/2\eta$ = 2.436 eV. The calculated values are shown in table 4. It is seen that the chemical potential of the title compound is negative and it means that the compound is stable. They do not decompose spontaneously into the elements they are made up of. The hardness signifies the resistance towards the deformation of electron cloud of chemical systems under small perturbation encountered during the chemical process. The principle of hardness works in chemistry and physics but it is not physically observable. Soft systems are large and highly polarizable, while hard systems are relatively small and are much less polarizable. NBO analysis provides the most accurate possible 'natural Lewis structure', because all orbital details are mathematically chosen to include the highest possible percentage of the electron density. A useful aspect of the NBO method is that it gives information about interactions in both filled and virtual orbital spaces that could enhance the analysis of intra- and intermolecular interactions. The NBO analysis of the cumene molecule was calculated by B3LYP method with 6-31++(d,p) basis set. The calculated values are given in Table 5.

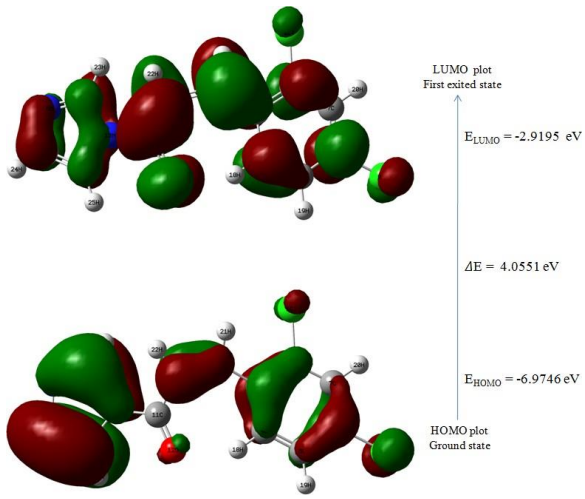

***Fig. 7**. Atomic orbital HOMO – LUMO composition of the frontier molecular orbital for (Z)-3- (2,4-dichlorophenyl)1-(1H-imidazol-1-yl)prop-2-en-1-one*

Table 4

Calculated energy values of (Z)-3-(2,4-dichlorophenyl)1-(1H-imidazol-1-yl)prop-2-en-1-one compound by B3LYP/6-311++G(d,p) method.

Basis set	B3LYP/6-311+G(d,p)
HOMO(eV)	-6.9746
LUMO(eV)	-2.9195
Ionization potential	6.9746
Electron affinity	2.9195
Energy gap(eV)	4.0551
Electronegativity	4.9471
Chemical potential	-4.9471
Chemical hardness	2.0276
Chemical softness	0.2466
Electrophilicity index	6.0352

Table 5

Second order perturbation theory analysis of Fock matrix in NBO basis for (Z)-3-(2,4-dichlorophenyl)1-(1H-imidazol-1-yl)prop-2-en-1-one.

[a]$E^{(2)}$ means energy of hyper conjugative interaction (stabilization energy)

[b]Energy difference between donor and acceptor i and j NBO orbitals.

[c]F(i,j) is the Fock matrix element between i and j NBO orbitals

Donor (i)	Type	ED /e	Acceptor(i)	Type	ED/e	[a]E(2) (KJ mol^{-1})	[b]E(J)-E(i) (a.u.)	[c]F(I,j) (a.u.)
Cl_1-C_2	Σ	1.98787	C_3-C_4	σ*	0.02568	2.81	1.3	0.054
			C_6-C_7	σ*	0.02978	2.06	1.3	0.046
C_2-C_3	Σ	1.9708	C_2-C_7	σ*	0.02775	3.87	1.3	0.063
			C_3-C_4	σ*	0.02568	4.38	1.28	0.067
C_2-C_3	Π	1.67074	C_4-C_5	π*	0.28023	17.02	0.31	0.066
			C_6-C_7	π*	0.38227	21.26	0.28	0.07
			C_9-C_{10}	π*	0.08876	6.31	0.29	0.041
C_2-C_7	Σ	1.97152	C_2-C_3	σ*	0.03906	4.56	1.29	0.069
			C_3-C_9	σ*	0.02599	3.49	1.19	0.058
			C_6-C_7	σ*	0.02978	4.24	1.3	0.066
			C_6-Cl_8	σ*	0.0288	4.17	0.89	0.055
C_3-C_4	Σ	1.96068	Cl_1-C_2	σ*	0.02863	4.56	0.86	0.056
			C_2-C_3	σ*	0.03906	5	1.26	0.071
C_3-C_9	Σ	1.97215	C_{10}-H_{22}	σ*	0.0173	3.26	1.09	0.053
C_4-C_5	Σ	1.96844	C_3-C_4	σ*	0.02568	3.4	1.27	0.059
			C_3-C_9	σ*	0.02599	3.7	1.17	0.059
			C_5-C_6	σ*	0.02899	4.17	1.28	0.065
C_4-C_5	π	1.67175	C_2-C_3	π*	0.41556	19.84	0.27	0.067
			C_6-C_7	π*	0.38227	22.51	0.27	0.07
C_4-H_{18}	σ	1.97807	C_2-C_3	σ*	0.03906	4.17	1.08	0.06
C_5-C_6	σ	1.97816	C_4-C_5	σ*	0.01651	3.68	1.33	0.062
C_5-H_{19}	σ	1.97689	C_3-C_4	σ*	0.02568	3.86	1.08	0.058
			C_6-C_7	σ*	0.02978	4.25	1.09	0.061
C_6-C_7	σ	1.97173	Cl_1-C_2	σ*	0.02863	4.51	0.88	0.056
			C_2-C_7	σ*	0.02775	4.3	1.3	0.067
C_6-C_7	π	1.69311	C_2-C_3	π*	0.41556	18.6	0.29	0.067
			C_4-C_5	π*	0.28023	17.25	0.31	0.066
C_7-H_{20}	σ	1.97518	C_2-C_3	σ*	0.03906	4.24	1.08	0.06
C_9-C_{10}	π	1.85728	C_{11}-O_{12}	π*	0.28081	25.59	0.29	0.08
C_{10}-C_{11}	σ	1.97497	C_9-C_{10}	σ*	0.01301	2.99	1.34	0.057
			N_{13}-C_{17}	σ*	0.0254	4.6	1.16	0.065
C_{10}-H_{22}	σ	1.97605	C_3-C_9	σ*	0.02599	4.42	1	0.059
			C_{11}-O_{12}	σ*	0.01494	4.12	1.14	0.061
			C_9-C_{10}	π*	0.08876	5.28	0.41	0.042
C_{14}-N_{15}	π	1.88029	C_{16}-C_{17}	π*	0.24419	21.29	0.35	0.079
C_{16}-C_{17}	π	1.84221	C_{14}-N_{15}	π*	0.32841	19.41	0.28	0.069
C_{l1}	LP (2)	1.96338	C_2-C_3	σ*	0.03906	4.4	0.88	0.056
			C_2-C_7	σ*	0.02775	4.55	0.9	0.057
C_{l1}	LP (3)	1.92191	C_2-C_3	π*	0.41556	13.17	0.34	0.065
Cl_8	LP (2)	1.96987	C_5-C_6	σ*	0.02899	4.32	0.89	0.055
			C_6-C_7	σ*	0.02978	4.68	0.89	0.058
Cl_8	LP (3)	1.91947	C_6-C_7	π*	0.38227	13.9	0.33	0.065
O_{12}	LP (2)	1.86953	C_{10}-C_{11}	σ*	0.05239	15.38	0.76	0.098
			C_{11}-N_{13}	σ*	0.07899	24.5	0.73	0.121
N_{13}	LP (1)	1.52902	C_{11}-O_{12}	π*	0.28081	55.31	0.28	0.118
			C_{14}-N_{15}	π*	0.32841	39.39	0.29	0.099
			C_{16}-C_{17}	π*	0.24419	26.44	0.32	0.087
	LP (	1.9238		σ*	0.04178	7.82	0.78	0.07

Molecular Electrostatic Potential (MEP) at a point in space around a molecule gives

information about the net electrostatic effect produced at that point by total charge distribution (electrons + protons) of the molecule and correlates with dipole moments, electro-negativity, partial charges and chemical reactivity of the molecules. It provides a visual method to understand the relative polarity of the molecule [19], [20]. An electron density isosurface mapped with electrostatic potential surface depicts the size, shape, charge density and site of chemical reactivity of themolecules. The MEP shown in Fig. 8 illustrates the charge distributions of the molecule three dimensionally. As it can be seen from Fig.8, the different values of the electrostatic potential at the surface are represented by different colours; red represents regions of most electronegative electrostatic potential, blue represents regions of the most positive electrostatic potential and green represents regions of zero potential. Potential increases in the order red < orange < yellow < green < blue. Blue indicates the strongest attraction and red indicates the strongest repulsion. Regions of negative potential are usually associated with the lone pair of electronegative atoms. As can be seen from the MEP map of the title molecule, negative region is mainly localized over the electronegative oxygen atoms, in the carbonyl group and the oxygen atom O_{12} of the methoxy group. The maximum positive region is localized on the phenyl rings. Further the MEP map of the title compound, show which of the regions having the negative potential are over the electro negative atoms, the regions having the positive potential are over the phenyl rings and the remaining species are surrounded by zero potential. From the MEP map, we can say that the phenyl rings atoms are sites for electrophilic attraction and O atoms are sites for nucleophilic activity.

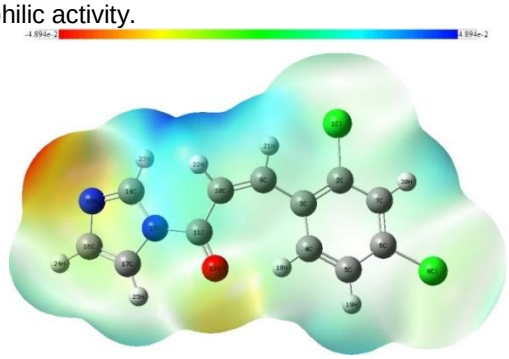

***Fig. 8**. Total electron density mapped with molecular electrostatic potential surface of (Z)-3-(2,4-dichlorophenyl)1-(1H-imidazol-1-yl)prop-2-en-1-one.*

3.5 Heat Treatment Effect

The total energy of a molecule is the sum of translational, rotational,vibrational and electronic energies. i.e., E = Et + Er + Ev + Ee. The statistical thermo - chemical analysis of the title molecule is carried out considering the molecule to be at room temperature of 298.15 K and one atmospheric pressure. The thermodynamic parameters, like rotational constant, zero point vibrational energy (ZPVE) of the molecule etc, are calculated by DFT method (B3LYP levels). The title molecule is considered as an asymmetric top having rotational symmetry number 1 and the total thermal energy has been arrived as the sum of electronic, translational, rotational and vibrational energies. The variations in the zero point vibrational energy (ZPVE) seem to be insignificant. The thermodynamic quantities such as entropy (S), heat capacity at constant pressure (Cp), enthalpy (H - E)/T, Gibb's free energy (G -E)/T and internal thermal energy (E) for various ranges (100–1000 K) of temperatures are determined and these results are presented in the Table 8. The correlation equations between these thermodynamic properties and temperatures were fitted by parabolic formula. All the thermodynamic data provide helpful information for the further study on the title compound. From the Table 8 it can be inferred that the thermodynamic parameters are increasing with temperature ranging from 100 K to 1000 K, due to the fact that the vibrational intensities of molecule with temperature. The following equations are used to predict approximately the values of heat capacity at constant pressure, entropy and internal energy for other range of temperature. The regression coefficient is also given in the parabolic equation.

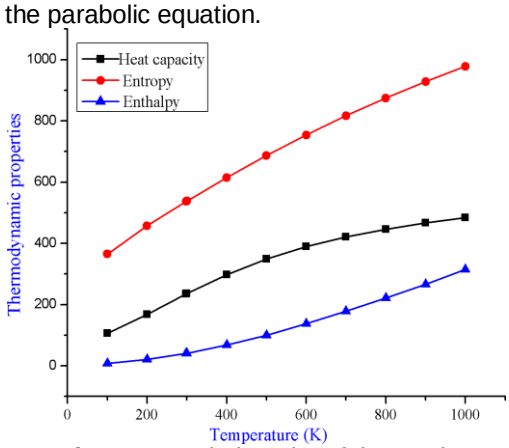

***Fig . 9**. Correlation plot of thermodynamic properties at different temperature of (Z)-3- (2,4-dichlorophenyl)1-(1H-imidazol-1-yl)prop-2-en-1-one compound*

Dipole moments reflect the molecular charge distribution and are given as a vector in three dimensions. Therefore, they can be used as descriptor to depict the charge movement across the molecule. Direction of the dipole moment vector in a molecule depends on the centers of positive and negative charges. Dipole moments are strictly determined for neutral molecule. For charged systems, their values depend on the choice of the origin and the molecular orientation. One of the important parameters of thermodynamics is the partition function. The partition function links thermodynamics, spectroscopy and quantum theory. The different types of partition functions are (i) translational partition function, (ii) rotational partition function, (iii) vibrational partition function and (iv) electronic partition function. Partition functions can be used to calculate heat capacities, entropies, equilibrium constants and rate constants. There are two ways to calculate the partition functions depending on the zero of energy to be either the bottom of the internuclear potential energy well, or the first vibrational level. If the zero reference point is set to be at the bottom of the well (BOT), then the overall vibrational partition function is calculated. On the other hand if the first vibrational energy level is set as the zero of energy (m = 0), then the overall partition function is calculated. Both of these are presented in the Table 6. The variation of the thermodynamic functions such as entropy, heat capacity, internal energy, enthalpy, and Gibb's free

energy with temperature are graphically represented in Fig. 9 respectively.

Table 6

Temperature dependence of the thermodynamic properties of (Z)-3-(2,4-dichlorophenyl)1-(1H-imidazol-1-yl)prop-2-en-1-one at B3LYP /6-311++G(d,P)

T(K)	$C^0_{p,m}$ (J/ mol K)	S^0_m (J/ mol K)	H^0_m (kJ/ mol)
100	105.957	364.897	7.242
200	168.514	457.188	20.913
298.15	234.371	536.743	40.684
300	235.593	538.196	41.119
400	297.438	614.667	67.849
500	348.486	686.733	100.24
600	388.9	753.989	137.19
700	420.838	816.431	177.738
800	446.436	874.357	221.147
900	467.304	928.185	266.868
1000	484.568	978.341	314.488

3.6 Non Linear Optical Activity

The molecules with large values of hyperpolarizabilities are more potential constituents of non-linear optical (NLO) materials, which find plentiful applications in the fields of physics, chemistry and engineering. The electric moments of a molecule are important quantities in structural chemistry. The dipole moment, polarizability and hyperpolarizability are characteristic features of a molecule in the presence of applied electric field [21]. When a molecule with permanent electric dipole moment □e(E) interacts with an external constant electrostatic field E, the change in the dipole moment can be written in tensor notation as

□e(E) = □e(0) + □ijEj + □ijk EjEk +....

Where,

□e(0) is the permanent dipole moment in the absence of electric field,

□e(E) is the dipole moment in the presence of the field,

□ij are the components those define the polarizability tensor,

□ijk are the components those define the first order hyperpolarizability. The values of total static dipole moment (□t), total polarizability (□t), anisotropy of polarizability (□□) and first order hyperpolarizability (□t) and its components of the molecules under investigation are evaluated using the equations that are available in literature [22], [23] to determine their NLO behavior by DFT employing B3LYP/6-33++G(d,p) basis set using Gaussian 09w program. The determination of □□component is very useful as it clearly specifies the direction of charge delocalization. The dominance of a component of □□in a particular direction substantiates the significant delocalization of charges in that direction. The large value of hyperpolarizability (□) along a particular direction is associated with the intra-molecular charge transfer, resulting from the electron cloud movement, through the □□conjugated frame work of electron [24]. From Table 7, it can be seen that the value of first order hyperpolarizability is large along $□_{xxx}$ in the molecules under investigation. This indicates that the □- electron delocalization has been extended towards $□_{xxx}$ direction and hence it is more enhanced for second harmonic generation along this direction. Such materials are suitable for growing crystals along this direction for NLO applications. Urea is an ideal molecule used in the NLO properties of molecular systems. Hence, the total molecular dipole moment (□t) 1.3732 Debye and the mean first order hyperpolarizability (□t) 0.3728 x 10-30 cm^5/esu of Urea are considered as threshold values for the purpose of comparison. The total molecular dipole moment (□t) values of the title molecule was calculated as 0.7853 Debye and the mean first order hyperpolarizability (□t) values were obtained and calculated as $13.5550X10^{-30}$ /esu. Thus,it can be seen that the values of dipole moment (□t) and first order hyperpolarizability (□t) of the titled molecules are greater than the threshold values of Urea. Hence, the title molecules may be considered as the potential applicants in the development of NLO materials based on the large value of the dipole moment and the first order hyperpolarizability.

Table 7

The values of calculated dipole moment□□ (D), polarizability ($□_0$), first order hyperpolarizability (βtot) components of (Z)-3-(2,4-dichlorophenyl)1-(1H-imidazol-1-yl)prop-2-en-1-one.

Parameters	B3LYP/ 6-311++ G(d,p)	Parameters	B3LYP /6-311++G(d,p)
□x	0.6069	β_{xxx}	-1545.9225
□y	0.1183	β_{xxy}	359.3970
□z	0.4842	β_{xyy}	-104.0437
□(D)	0.7853	β_{yyy}	55.1013
□xx	306.3632	β_{zxx}	110.1636
□xy	-11.8126	β_{xyz}	17.9658
□yy	190.3692	β_{zyy}	71.0161
□xz	-3.8475	β_{xzz}	156.4012
□yz	-2.6372	β_{yzz}	39.9001
□zz	106.2540	β_{zzz}	-24.7396
□□□e.s.u□	2.9788×10^{-23}	βtot (e.s.u)	13.5550×10^{-30}
Δ□□e.s.u□	8.2762×10^{-23}		

3.7 Antibacterial Activity and Antifungal Activity

Various aspects of pharmacological behavior and biological characteristics of a material can be evaluated based on. The title molecule was screened for its in vitro antimicrobial activity against bacterial stains by agar well diffusion method [25], [26]. The antibacterial activity of the compound was tested against Escherichia coli and Staphylococcus aureus at three different concentrations and DMSO was used as positive control. It is to be noted that the solvent itself has no activity on the microbes and antibacterial activity is dose dependent. The inhibitory activity of the of (Z)-3-(2,4-dichlorophenyl)1-(1H-imidazol-1-yl)prop-2-en-1-one on the organisms is high activity at higher concentration of 100 µl. The compound has significant antibacterial activity as compared to that of standard kanamycin. The antimicrobial activity and solvent sensitivity of the title molecule are presented in Table 9. The in vitro antifungal activity of (Z)-3-(2,4-dichlorophenyl)1-(1H-imidazol-1-yl)prop-2-en-1-one was evaluated against three fungal strains, namely, Candida albicans, A.niger and Trichophyton at different concentrations. Table 9 illustrates the antimicrobial activity of the titled molecule. The data indicate that the compound shows good antifungal activity against the tested microorganisms, at 100 µl concentration when compared to that of standard clotrimazole. The results clearly indicate that as the concentration of the compound increases, the inhibition of fungal strains also increases. Antibacterial and antifungal activities of (Z)-3-(2,4-dichlorophenyl)1-(1H-imidazol-1-yl)prop-2-en-1-one are given in Table 8. The antibacterial and antifungal activities are shown in Fig. 10

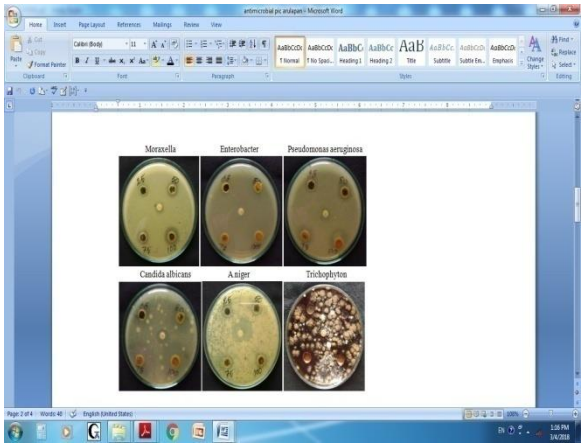

***Fig. 10**. Antibacterial activity and antifungal activity of (Z)-3-(2,4-dichlorophenyl)1-(1H- imidazol-1-yl)prop-2-en-1-one molecule*

Table 8

Antimicrobial activity of (Z)-3-(2,4-dichlorophenyl)1-(1H-imidazol-1-yl)prop-2-en-1-one.

ORGANISM	DMSO Extract added and Zone of inhibition (mm/ml)				
	Control	25 µl	50 µl	75 µl	100 µl
Moraxella	12	10	20	25	32
Enterobacter	16	13	17	21	25
Pseudomonas aeruginosa	12	12	16	20	26
Candida albicans	15	15	20	25	30
A.niger	10	12	20	27	36
Trichophyton	10	20	25	35	40

4 CONCLUSION

In this work, we have performed the experimental and theoretical vibrational analysis of ((Z)-3-(2,4-dichlorophenyl)-1-(1H-imidazol-1-yl)prop-2-en-1-one (1). The molecular geometry, vibrational frequencies, FT-IR and FT-Raman spectra of the molecule in the ground state are calculated by using DFT (B3LYP) method 6-311++G(d,p) basis set. The vibrational wavenumbers are calculated and the complete assignments are performed on the basis of the PED of the vibrational modes. The results are compared with experimental FT-IR and FT-Raman spectra. The correlation graphic is plotted to see the harmony between the calculated and experimental wavenumbers and the graphic showed a very good coherence with FT-IR results. Nonlinear optical (NLO) behaviour of the title molecule has been investigated by the dipole moment, the polarizability and the first order hyperpolarizability. HOMO-LUMO gap is calculated as 4.0071eV. Additionally, the thermodynamic and the electronic properties of the tittle compound are calculated. Using NBO analysis the stability of the molecule arising

from hyper-conjugative interaction and charge delocalization has been analyzed. In short, this study made for ((Z)-3-(2,4-dichlorophenyl)-1-(1H-imidazol-1-yl)prop-2-en-1-one (1) gives a comprehensive view related to the geometry, vibrational properties (based on FT-IR, FT-Raman), NLO, HOMO-LUMO, NBO, MEP and thermodynamic properties.

REFERENCES

[1] Arunkumar S Suvarna, "Research Journal of Chemical Sciences" 5(10) 67-72, (2015).

[2] M.J. Frisch, G.W. Trucks, H.B. Schlegel, G.E. Scuseria, M.A. Robb,J.R. Cheeseman, G. Scalmani, V. Barone, B. Mennucci, G.A. Petersson,H. Nakatsuji, M. Caricato, X. Li, H.P. Hratchian, A.F. Izmaylov, J. Bloino,G. Zheng, J.L. Sonnenberg, M. Hada, M. Ehara, K. Toyota, R. Fukuda,J. Hasegawa, M. Ishida, T. Nakajima, Y. Honda, O. Kitao, H. Nakai, T. Vreven,J.A. Montgomery Jr., J.E. Peralta, F. Ogliaro, M. Bearpark, J.J. Heyd, E. Brothers,K.N. Kudin, V.N. Staroverov, R. Kobayashi, J. Normand, K. Raghavachari,A. Rendell, J.C. Burant, S.S. Iyengar, J. Tomasi, M. Cossi, N. Rega, J.M. Millam,M. Klene, J.E. Knox, J.B. Cross, V. Bakken, C. Adamo, J. Jaramillo, R. Gomperts,R.E. Stratmann, O. Yazyev, A.J. Austin, R. Cammi, C. Pomelli, J.W. Ochterski,R.L. Martin, K. Morokuma, V.G. Zakrzewski, G.A. Voth, P. Salvador,J.J. Dannenberg, S. Dapprich, A.D. Daniels, €O. Farkas, J.B. Foresman, J.V. Ortiz,J.Cioslowski, D.J. Fox, Gaussian 09, Revision E.01, Gaussian, Inc., WallingfordCT, (2009).

[3] GaussView, Version 5, Roy Dennington, Todd Keith, and John Millam, SemichemInc., Shawnee Mission, KS, (2009).

[4] M.H. Jomroz, Vibrational Energy Distribution Analysis,VEDA4, (2004). Warsaw.

[5] K. Wolinski, R. Haacke, J.F. Hinton, P. Pulay, "Methods for parallel computationof SCF NMR chemical shifts by GIAO method: efficient integral calculation,multi-Fock algorithm, and pseudodiagonalization, J. Comp. Chem". 18 (6) 816-825, (1997).

[6] G. Keresztury, S. Holly, J. Varga, G. Besenyei, A.Y. Wang, J.R. During, "Vibrationalspectra of monothiocarbamates-II. IR and Raman spectra, vibrational assignment,conformational analysis and ab initio calculations of S-methyl-N,Ndimethylthiocarbamate",Spectrochim. Acta A 49 (1993) 2007-2026.

[7] G. Keresztury, in: J.M. Chalmers, P.R. Griffith (Eds.), "Raman Spectroscopy":Theory in Hand Book of Vibrational Spectroscopy, vol. 1, John Wiley& SonsLtd, New York, (2002).

[8] G.Socrates, "Infrared Characteristic Group Frequencies", Wiley, Interscience Publications, NewYork, (1980).M.Silverstein, G.GlaytonBasseler, C.Morill, "Spectrometric Identification of OrganicCompounds", Wiley, New York, (1981).

[9] M.Arivazhagan, K.Sambathkumar, S.Jeyavijayan, Indian J.Pure& Appl. Phys. 48, 869-874, (2010).

[10] R.J. Anderson, D.J. Bendell, P.W. Groundwater, "Organic Spectroscopic Analysis", The RoyalSociety of Chemistry (RSC) Sunderland, England, (2004).D.L. Pavia, G.M. Lampman, G.S. Kriz, J.R. Vyvyan, "Introduction to Spectroscopy",Brooks/Cole Cengage Learning, USA, (2009).

[11] J.B. Lambert, H.F. Shurvell, R.G. Cooks. "Introduction to Organic Spectroscopy", Macmillan Publish, NewYork, USA, (1987).

[12] P. Politzer, P.R. Laurence, K. Jayasuriya, J. McKinney, Environ. Health Perspect.61, 191–202, (1985).

[13] I. Fleming, Frontier Orbitals, "Organic Chemical Reactions", John Wiley and Sons, New York, (1976).

[14] T.A. Koopmans, Physica 1,104–113, (1993).

[15] R.J. Parr, L.V. Szentpaly, S. Liu, J. Am. Chem. Soc. 121, 1922–1924, (1999).

[16] R.J. Parr, R.G. Pearson, J. Am. Chem. Soc. 105,7512–7516, (1983).

[17] S. Chidangil, M.K. Shukla, P.C. Mishra, J. Mol. Model 4, 250–258, (1998).

[18] F.J. Luque, J.M. Lopez, M. Orozco, Theor. Chem. Acc. 103, 343–345, (2000).

[19] A. Hinchliffe, R.W. Munn, "Molecular Electromagnetism", John Wiley and Sons Ltd: Chichester(1985).

[20] D. A. Klienman, Phys. Rev. 126, 1977, 1962).

[21] R. Zhang, B. Du, G. Sun, Y. X. Sun, Spectrochim. Acta A, 75,1115, (2002).

[22] C. H. Choi, M. Kertez., J. Phys. Chem A. 101(1997)3821-3831

[23] B. Lillian, R. Calhelha, I. Ferreira, P. Baptista, L. Estevinho, Eur. Food Res.Technol. 225 151-156, (2007).

[24] A.H. Collins (Ed.), "Microbiology Method", second ed., Butterworth, London, (1976).